

Shear softening in tantalum at megabar pressuresDaniele Antonangeli,^{1,2} Daniel L. Farber,^{1,3} Ayman H. Said,⁴ Laura Robin Benedetti,^{1,5} Chantel M. Aracne,¹ Alexander Landa,¹ Per Söderlind,¹ and John E. Klepeis¹¹*Lawrence Livermore National Laboratory, Livermore, California 94550, USA*²*Institut de Minéralogie et de Physique des Milieux Condensés, UMR CNRS 7590, Institut de Physique du Globe de Paris, Université Pierre et Marie Curie, Université Paris Diderot, 75005 Paris, France*³*Department of Earth and Planetary Sciences, University of California–Santa Cruz, Santa Cruz, California 95064, USA*⁴*Advanced Photon Source, Argonne National Laboratory, Argonne, Illinois 60192, USA*⁵*Department of Earth and Planetary Sciences, University of California–Berkeley, Berkeley, California 94720, USA*

(Received 13 July 2010; revised manuscript received 6 September 2010; published 4 October 2010)

We have experimentally and theoretically investigated the aggregate elasticity of tantalum to pressures exceeding 1 Mbar. Our inelastic x-ray scattering measurements show a softening in the aggregate shear velocity in the 90–100 GPa range with typical pressure dependence above 120 GPa. Our calculations suggest that, in analogy with theoretical predictions on vanadium and niobium, this anomalous behavior is likely due to the intraband nesting of the Fermi surface that leads to an electronic topological transition and a concomitant transverse-acoustic-phonon mode softening.

DOI: [10.1103/PhysRevB.82.132101](https://doi.org/10.1103/PhysRevB.82.132101)

PACS number(s): 62.50.–p, 62.30.+d, 63.20.kd, 64.70.kd

Since the pioneering works of Bridgman in the 1950s,¹ it has been known that yield strength and ductility, as well as the elasticity of metals are strongly affected by even moderate pressures. Understanding the physics underlying increases in material strength under compression is important to a broad range of scientific fields such as material science, solid-state physics, and geophysics and planetary physics.

Consequently, a great deal of effort has been put into the experimental investigation and theoretical descriptions of the mechanical properties of materials under extreme conditions. Tantalum, which is bcc at room pressure and temperature, is predicted to retain the bcc structure over a very large pressures and temperature range.² Thus, it is one of the most widely used benchmarks for the study of yield strength and for testing theoretical predictions of elastic and plastic behavior under extreme conditions.^{3–9} However, both experimental and theoretical descriptions of plasticity, from the atomistic scale to the macroscopic stress-strain conditions, require accurate descriptions of the elastic properties at high pressure (cf. Ref. 7).

Further interest in the elastic properties of Ta under compression comes from theoretical predictions^{10,11} of an electronic topological transition¹² that drives an anomalous behavior of the elastic modulus C_{44} above megabar (Mbar) pressure. Conceptually similar phenomena have been invoked to explain the observed rhombohedral distortion that occurs in vanadium¹³ and the temperature dependence of the elastic moduli of niobium.¹⁴ However, while theory suggests that this is a general feature of group VB elements,^{11,15–17} no experiments have indicated the presence of an anomalous softening of the transverse-acoustic phonons in Ta.

At present, there exist ultrasonic determinations of the elastic moduli of tantalum up to 0.5 GPa,¹⁸ impulsive stimulated light scattering (ISLS) results to 30 GPa,¹⁹ radial x-ray diffraction measurements (RXRD) to 105 GPa,²⁰ and theoretical calculations.^{2,10,11,21} Partial information on the elastic properties can also be inferred from the experimentally determined equation of state (EOS).^{22,23} Unfortunately, at pres-

ures above 20 GPa, there is significant disagreement between these determinations and likely the most reliable results are provided by extrapolation of the ultrasonic work. However, a simple extrapolation of low-pressure data results in uncertainties of $\sim 20\%$ at 1 Mbar,⁷ and a clear hindrance to the search for any anomalous mode softening.

Here we present experimental and theoretical constraints on the elasticity of Ta at pressures exceeding the Mbar, mainly focusing on the aggregate properties. Indeed, while inelastic x-ray scattering (IXS) has been proven a powerful tool for the investigation of single-crystalline elasticity at high pressure and high temperature,^{24,25} as well for the investigation of the electron-phonon coupling,^{26,27} the extension of IXS measurement on single crystals to Mbar pressures is greatly limited by the severe constraints imposed on the sample size and quality. Accordingly, to be able to cover the largest pressure range, we performed our measurements on polycrystalline samples. The samples consisted of commercially available, high-purity (99.999%) tantalum powder loaded without pressure-transmitting medium in a membrane-driven diamond-anvil cell equipped with 300/150 μm single bevel diamonds and a rhenium gasket.

The experiments were carried out at the high-energy resolution inelastic x-ray scattering spectrometer (HERIX) at sector 30 at the Advanced Photon Source. The synchrotron beam was monochromatized by a diamond double-crystal monochromator to 1.6 eV at 23.724 keV, and then to 1 meV bandwidth using a six-reflection crystal inline monochromator. The energy scans were performed by rotating crystals. The beam was focused by a Kirkpatrick-Baez mirror to a spot size of 35 m horizontally and 15 m vertically and the scattered radiation from the sample was collected at 9 m distance by silicon analyzers in backscattering geometry using the Si [12 12 12] reflection. The overall energy resolution was 1.5 meV full width at half maximum. Spectra have been collected in transmission geometry, with the x-ray beam impinging on the sample through the diamonds, along the main compression axis of the cell, and hence probing exchange momenta q almost perpendicular to the cell axis. In parallel

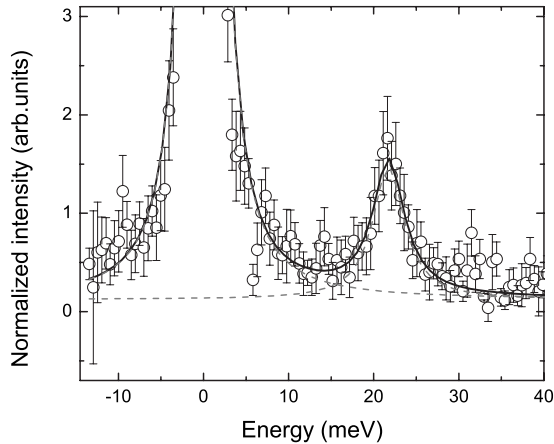


FIG. 1. IXS spectrum collected at ambient temperature and 120 GPa, for $q=6 \text{ nm}^{-1}$. The experimental data and their statistical error bars are shown together with the best fits.

to the IXS measurements we also collected Ta diffraction lines to directly determine the density ρ and thus the pressure by using tantalum EOS.²³ We collected data at 0.4, 1, 43, 68, 88, 96, and 120 GPa, constraining the aggregate longitudinal phonon dispersion by 4–5 IXS spectra collected in the 4–16 nm^{-1} range. The energy of the phonons was extracted by fitting a set of Lorentzian functions to the IXS spectra, utilizing a standard χ^2 minimization routine. An example of the IXS spectra and fit obtained at 120 GPa is shown in Fig. 1.

We determined the aggregate longitudinal sound velocity V_L by fitting a sinus function to the experimentally determined phonon dispersions (Born–von Karman lattice-dynamics theory limited to the first neighbor interaction),^{28,29} with typical indetermination of $\pm 2\text{--}3\%$. Combining our measurements of V_L and ρ with the adiabatic bulk modulus K ($\sim 1\%$ correction to the isothermal values²³), we can obtain the aggregate shear sound velocities V_S from the relation $V_S = [3/4(V_L^2 - K/\rho)]^{1/2}$. This approach results in somewhat larger uncertainties (typical errors $\sim 4\text{--}5\%$, up to 7%) in V_S due to error propagation. Detailed discussion on the link between the longitudinal-acoustic-phonon dispersion probed by IXS technique in polycrystalline materials, the aggregate macroscopic velocities and the average of single-crystal moduli, in particular, on textured samples, can be found elsewhere.^{30,31}

Our computational method is based on the first-principles density-functional theory and yields the total energy of a periodic system without any experimental input. In principle, this only involves one approximation, namely, the assumed form of the density functional for the exchange and correlation energy of the electrons, which here is the generalized gradient approximation.³² However, in practice other approximations are often included with any actual computational method. In the present work, we have made a special effort to remove such additional approximations. Specifically: (i) the electron charge density and the one-electron potential are allowed to have any geometrical shape; (ii) all relativistic terms, except the spin-orbit coupling (which has a small effect²¹), are included; and (iii) the numerical basis set

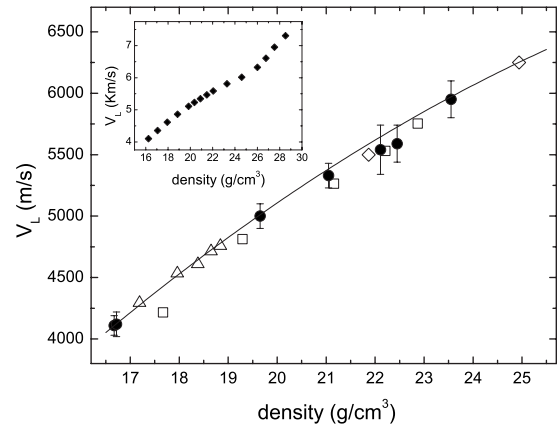


FIG. 2. Aggregate longitudinal sound velocity as a function of density. Solid circles, IXS measurements; open triangles, ISLS (Ref. 19); open squares, RXRD (Ref. 20); and open diamonds, shock-wave compression (Ref. 34). The solid line is the extrapolation of the ultrasonic measurements (Ref. 18) [relative uncertainty $\sim 20\%$ at 1 Mbar (Ref. 7)]. Inset: computational results (Voigt-Reuss-Hill average).

used is extended to a so-called “double basis” set in order to minimize truncation errors in the expansion of the one-electron wave functions. The present method incorporates nonsphericity to the charge density and potential by representing the crystal with nonoverlapping spheres (of a variable, optimum size) surrounding each atomic site and a general shaped interstitial region between the spheres. Inside the spheres, the wave functions are represented as Bloch sums of linear muffin-tin orbitals and are expanded by means of structure constants. The kinetic energy is not restricted to be zero in the interstitial region and the wave-function expansion contains Hankel and Neumann functions (depending on sign of the kinetic energy) together with Bessel functions. The analytical expressions for these expansions can be found elsewhere.³³ In order to represent the wave functions in Ta as accurately as possible we have defined here, in a single energy panel, $5s$, $5p$, and $4f$ semicore states and $6s$, $6p$, $5d$, and $5f$ valence states. The aforementioned “double basis set” is applied, i.e., two kinetic-energy parameters (κ^2) appropriate for the tails of each state.

The experimentally measured aggregate longitudinal and shear sound velocities are shown as a function of density in Figs. 2 and 3, together with previous determinations obtained by different techniques. In the case of V_L , all results are in overall good agreement with the values obtained from radial diffraction measurements²⁰ being somewhat slower than the other data sets. In particular, the IXS results are in excellent agreement with ultrasonic determination at low pressure¹⁸ and the shock wave determination at high pressure.³⁴

For V_S , our experimental results compare favorably with ultrasonic low-pressure values. The ISLS results are only somewhat slower than IXS while the deviation of the RXRD results from the other data is quite significant. This discrepancy likely arises due to the limitations in the model used to derive the elastic moduli from radial diffraction results. Indeed the assumption that there exists a single uniform macroscopic stress applied to all grains in the polycrystal is vio-

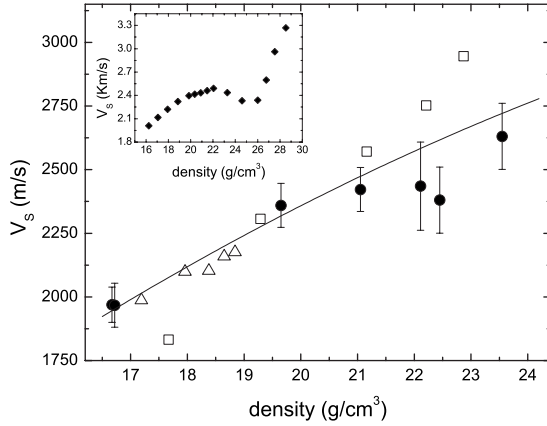


FIG. 3. Aggregate shear sound velocity as a function of density. Solid circles, IXS measurements; open triangles, ISLS (Ref. 19); open squares, RXRD (Ref. 20). The solid line is the extrapolation of the ultrasonic measurements (Ref. 18) [relative uncertainty $\sim 20\%$ at 1 Mbar (Ref. 7)]. Inset: computational results (Voigt-Reuss-Hill average).

lated in cases where there is plastic deformation, so that the “apparent” elastic moduli deduced from x-ray diffraction under Reuss or geometric averages consistently differ from those measured on single crystals.^{35,36} Up to about $21.05 \text{ g/cm}^3 \leftrightarrow 68 \text{ GPa}$, the extrapolation of the ultrasonic measurements holds suitably well. Above this density, in the relatively narrow density (pressure) range between 22.11 and 22.45 g/cm^3 ($88\text{--}96 \text{ GPa}$), we observe a distinct softening of V_S , that is almost completely recovered by $\rho = 23.55 \text{ g/cm}^3 \leftrightarrow 120 \text{ GPa}$. We note, that even if much smaller in magnitude and within the experimental error bars, the same qualitative behavior can be seen in V_L over this density (pressure) region.

The effects of texture alone can account for differences between IXS results on polycrystalline samples and orientation-averaged single-crystal moduli but only up to few percent even in case of highly anisotropic materials.^{28,30} We point out, that the high crystal symmetry of Ta (bcc) makes it a quite favorable case and that the observed softening of V_S is more than 9%, an amount significantly larger even than the 3% expected as a consequence of the developed preferential alignment at similar pressures for the critical case of hcp-Co.³⁰ Moreover, the effect of texture is either a continuous smooth function of pressure³⁰ or levels out when texture saturates.^{35,37} Thus, it is highly unlikely that developed preferential alignment can account for the localized softening over a narrow pressure range that we document.

The qualitative agreement between the IXS measurements and the calculations (see insets of Figs. 2 and 3), which well capture the small anomaly in V_L and the distinct softening of V_S (although at higher density), suggest that at the origin of the observed density/pressure evolution there is the progressive intraband nesting of the Fermi surface that eventually leads to transverse-acoustic-phonon mode softening. Indeed,

with increasing pressure, the s -derived bands shift higher in energy relative to the d -derived bands (s -to- d transition³⁸). At a critical pressure, specific features in the electronic band structure move into close vicinity of the Fermi level. The reduced symmetry of the C_{44} shear distortion splits degeneracies associated with these features in the electronic bands, leading to an energy gain as a function of the distortion. This energy gain at least partially counterbalances the standard elastic strain energy cost, resulting in an anomalous softening of the elastic response. As the pressure is increased further the relevant features in the band structure shift away from the Fermi level, restoring the standard behavior as a function of the shear distortion.

This volume-dependent softening of the transverse-acoustic phonons has been predicted by theory as a general feature of all group V metals^{11,15–17,39–41} but had not been experimentally documented for Ta. Indeed, as the topology of the electronic band structure near the Fermi level is very similar for each of the group V transition metals, theoretical considerations suggest a common origin for the pressure-induced shear softening reported here for tantalum, the anomalous softening of the elastic moduli of niobium at high temperature¹⁴ and the bcc-to-rhombohedral phase transition in vanadium.¹³ The effect is present in all the group VB elements, but most pronounced in period 4 (V), and decreases in magnitude to period 6 (Ta). Thus, only in the case of vanadium the energy gain seems large enough to produce a structural phase transition.

Finally, with the exception of the relatively narrow pressure range where the electronic topological transition occurs, the single-crystalline elastic tensor of Ta at very high pressure is well described by the relation

$$C_{ij}(P) = C_{ij}(P=0) + \frac{dC_{ij}}{dP}(P=0)P\left(\frac{V}{V_0}\right)^{1/3}$$

with the values of the individual C_{ij} at $P=0$ (ambient) and the pressure derivative dC_{ij}/dP fixed to the ones obtained by ultrasonic techniques.¹⁸ Such a good agreement, although *a priori* nonobvious, does not come totally unexpected, as a quite remarkable agreement between the extrapolation of the volume-pressure relation determined by ultrasonic and shock-wave isotherm (at 300 K) has already been observed.¹⁸ These considerations reinforce the notion of tantalum as prototype metal for the investigation and calibration of equation of state and material strength at extreme thermodynamics conditions.

This work was performed under the auspice of the U.S. DOE by LLNL under Contract No. DE-AC52-07NA27344. Use of the Advanced Photon Source was supported by the U.S. Department of Energy, Office of Science, Office of Basic Energy Sciences, under Contract No. DEAC02-06CH11357. The construction of HERIX was partially supported by the NSF under Grant No. DMR-0115852.

- ¹P. Bridgman, *J. Appl. Phys.* **24**, 560 (1953).
- ²D. Orlikowski, P. Söderlind, and J. A. Moriarty, *Phys. Rev. B* **74**, 054109 (2006).
- ³D. J. Steinberg, S. G. Cochran, and M. W. Guinan, *J. Appl. Phys.* **51**, 1498 (1980).
- ⁴S. T. Weir, J. Akella, C. Ruddle, T. Goodwin, and L. Hsiung, *Phys. Rev. B* **58**, 11258 (1998).
- ⁵G. Wang, A. Strachan, T. Cagin, and W. A. Goddard III, *Phys. Rev. B* **67**, 140101(R) (2003).
- ⁶L. H. Yang, P. Söderlind, and J. A. Moriarty, *Philos. Mag. A* **81**, 1355 (2001).
- ⁷A. Dewaele and P. Loubeyre, *Phys. Rev. B* **72**, 134106 (2005).
- ⁸Z. L. Liu, L. C. Cai, X. R. Chen, Q. Wu, and F. Q. Jing, *J. Phys.: Condens. Matter* **21**, 095408 (2009).
- ⁹T. J. Vogler, *J. Appl. Phys.* **106**, 053530 (2009).
- ¹⁰O. Gülseren and R. E. Cohen, *Phys. Rev. B* **65**, 064103 (2002).
- ¹¹L. Koči, Y. Ma, A. R. Oganov, P. Souvatzis, and R. Ahuja, *Phys. Rev. B* **77**, 214101 (2008).
- ¹²I. M. Lifshitz, *Sov. Phys. JETP* **11**, 1130 (1960).
- ¹³Y. Ding, R. Ahuja, J. Shu, P. Chow, W. Luo, and H. K. Mao, *Phys. Rev. Lett.* **98**, 085502 (2007).
- ¹⁴Y. Talmor, E. Walker, and S. Steinemann, *Solid State Commun.* **23**, 649 (1977).
- ¹⁵A. Landa, J. Klepeis, P. Söderlind, I. Naumov, O. Velikokhatnyi, L. Vitos, and A. Ruban, *J. Phys. Chem. Solids* **67**, 2056 (2006).
- ¹⁶A. Landa, J. Klepeis, P. Söderlind, I. Naumov, O. Velikokhatnyi, L. Vitos, and A. Ruban, *J. Phys.: Condens. Matter* **18**, 5079 (2006).
- ¹⁷A. Landa, P. Söderlind, A. V. Ruban, O. E. Peil, and L. Vitos, *Phys. Rev. Lett.* **103**, 235501 (2009).
- ¹⁸K. Katahara, M. H. Manghnani, and E. S. Fisher, *J. Appl. Phys.* **47**, 434 (1976).
- ¹⁹J. C. Crowhurst, J. M. Zaug, E. H. Abramson, J. M. Brown, and D. W. Ahre, *High Press. Res.* **23**, 373 (2003).
- ²⁰H. Cynn and C. S. Yoo (unpublished).
- ²¹P. Söderlind and J. A. Moriarty, *Phys. Rev. B* **57**, 10340 (1998).
- ²²H. Cynn and C. S. Yoo, *Phys. Rev. B* **59**, 8526 (1999).
- ²³A. Dewaele, P. Loubeyre, and M. Mezouar, *Phys. Rev. B* **70**, 094112 (2004).
- ²⁴D. Antonangeli, M. Krisch, G. Fiquet, D. L. Farber, C. M. Aracne, J. Badro, F. Occelli, and H. Requardt, *Phys. Rev. Lett.* **93**, 215505 (2004).
- ²⁵D. Antonangeli, M. Krisch, D. L. Farber, D. G. Ruddle, and G. Fiquet, *Phys. Rev. Lett.* **100**, 085501 (2008).
- ²⁶D. L. Farber, M. Krisch, D. Antonangeli, A. Beraud, J. Badro, F. Occelli, and D. Orlikowski, *Phys. Rev. Lett.* **96**, 115502 (2006).
- ²⁷A. Bosak, M. Hoesch, D. Antonangeli, D. L. Farber, I. Fischer, and M. Krisch, *Phys. Rev. B* **78**, 020301(R) (2008).
- ²⁸D. Antonangeli, F. Occelli, H. Requardt, J. Badro, G. Fiquet, and M. Krisch, *Earth Planet. Sci. Lett.* **225**, 243 (2004).
- ²⁹D. Antonangeli, M. Krisch, G. Fiquet, J. Badro, D. L. Farber, A. Bossak, and S. Merkel, *Phys. Rev. B* **72**, 134303 (2005).
- ³⁰A. Bosak, M. Krisch, I. Fischer, S. Huotari, and G. Monaco, *Phys. Rev. B* **75**, 064106 (2007).
- ³¹D. Antonangeli, J. Siebert, J. Badro, D. L. Farber, G. Fiquet, G. Morard, and F. J. Ryerson, *Earth Planet. Sci. Lett.* **295**, 292 (2010).
- ³²J. P. Perdew, J. A. Chevary, S. H. Vosko, K. A. Jackson, M. R. Pederson, D. J. Singh, and C. Fiolhais, *Phys. Rev. B* **46**, 6671 (1992).
- ³³J. M. Wills, O. Eriksson, M. Alouani, and D. L. Price, in *Electronic Structure and Physical Properties of Solids*, edited by H. Dreyse (Springer-Verlag, Berlin, 1998), p. 148.
- ³⁴J. M. Brown and J. W. Shaner, in *Shock Waves in Condensed Matter—1983*, edited by J. R. Asay *et al.* (Elsevier, New York, 1984), p. 91.
- ³⁵S. Merkel, N. Miyajima, D. Antonangeli, G. Fiquet, and T. Yagi, *J. Appl. Phys.* **100**, 023510 (2006).
- ³⁶D. Antonangeli, S. Merkel, and D. L. Farber, *Geophys. Res. Lett.* **33**, L24303 (2006).
- ³⁷S. Merkel, C. Tomé, and H.-R. Wenk, *Phys. Rev. B* **79**, 064110 (2009).
- ³⁸A. K. McMahan, *Physica B & C* **139-140**, 31 (1986).
- ³⁹N. Suzuki and M. Otani, *J. Phys.: Condens. Matter* **14**, 10869 (2002).
- ⁴⁰B. Lee, R. E. Rudd, J. E. Klepeis, P. Söderlind, and A. Landa, *Phys. Rev. B* **75**, 180101(R) (2007).
- ⁴¹B. Lee, R. E. Rudd, J. E. Klepeis, and R. Becker, *Phys. Rev. B* **77**, 134105 (2008).